ISSN 1674-1056
http://cpb.iphy.ac.cn
http://iopscience.iop.org/cpb
中国物理 B
Chinese Physics
中国物理 Chinese Physics B

Effect of P impurity on mechanical properties of NiAl ∑5 grain boundary: From perspectives of stress and energy

Xue-Lan Hu(胡雪兰), Ruo-Xi Zhao(赵若汐), Jiang-Ge Deng(邓江革), Yan-Min Hu(胡艳敏), Qing-Gong Song(宋庆功)
Citation: Chin. Phys. B . 2018, 27(3): 037105. **doi:** 10.1088/1674-1056/27/3/037105

Journal homepage: http://cpb.iphy.ac.cn; http://iopscience.iop.org/cpb

What follows is a list of articles you may be interested in

Effect of P impurity on NiAlΣ5 grain boundary from first-principles study

Xue-Lan Hu(胡雪兰), Ruo-Xi Zhao(赵若汐), Yang Luo(罗阳), Qing-Gong Song(宋庆功)
Chin. Phys. B . 2017, 26(2): 023101. **doi:** 10.1088/1674-1056/26/2/023101

First-principles study of the effects of selected interstitial atoms on the generalized stacking fault energies, strength, and ductility of Ni

Li Chun-Xia, Dang Sui-Hu, Wang Li-Ping, Zhang Cai-Li, Han Pei-De
Chin. Phys. B . 2014, 23(11): 117102. **doi:** 10.1088/1674-1056/23/11/117102

Investigations of the half-metallic behavior and the magnetic and thermodynamic properties of half-Heusler CoMnTe and RuMnTe compounds：A first-principles study

T. Djaafri, A. Djaafri, A. Elias, G. Murtaza, R. Khenata, R. Ahmed, S. Bin Omran, D. Rached
Chin. Phys. B . 2014, 23(8): 087103. **doi:** 10.1088/1674-1056/23/8/087103

The structural, elastic, and electronic properties of $Zr_xNb_{1-x}C$ alloys from first principle calculations

Sun Xiao-Wei, Zhang Xin-Yu, Zhang Su-Hong, Zhu Yan, Wang Li-Min, Zhang Shi-Liang, Ma Ming-Zhen, Liu Ri-Ping
Chin. Phys. B . 2013, 22(10): 107105. **doi:** 10.1088/1674-1056/22/10/107105

First-principles investigation on the structural and elastic properties of *cubic*-Fe_2TiAl under high pressures

Liu Xian-Kun, Liu Cong, Zheng Zhou, Lan Xiao-Hua
Chin. Phys. B . 2013, 22(8): 087102. **doi:** 10.1088/1674-1056/22/8/087102

Effect of P impurity on mechanical properties of NiAl Σ5 grain boundary: From perspectives of stress and energy*

Xue-Lan Hu(胡雪兰)[1,†], Ruo-Xi Zhao(赵若汐)[1], Jiang-Ge Deng(邓江革)[1], Yan-Min Hu(胡艳敏)[1], and Qing-Gong Song(宋庆功)[2]

[1] *Sino-European Institute of Aviation Engineering, Civil Aviation University of China, Tianjin* 300300, *China*
[2] *College of Science, Civil Aviation University of China, Tianjin* 300300, *China*

(Received 29 October 2017; revised manuscript received 20 December 2017; published online 13 February 2018)

In this paper, we employ the first-principle total energy method to investigate the effect of P impurity on mechanical properties of NiAl grain boundary (GB). According to "energy", the segregation of P atom in NiAlΣ5 GB reduces the cleavage energy and embrittlement potential, demonstrating that P impurity embrittles NiAlΣ5 GB. The first-principle computational tensile test is conducted to determine the theoretical tensile strength of NiAlΣ5 GB. It is demonstrated that the maximum ideal tensile strength of NiAlΣ5 GB with P atom segregation is 144.5 GPa, which is lower than that of the pure NiAlΣ5 GB (164.7 GPa). It is indicated that the segregation of P weakens the theoretical strength of NiAlΣ5 GB. The analysis of atomic configuration shows that the GB fracture is caused by the interfacial bond breaking. Moreover, P is identified to weaken the interactions between Al–Al bonds and enhance Ni–Ni bonds.

Keywords: NiAlΣ5 grain boundary, P impurity, first principles, mechanical properties

PACS: 71.20.Lp, 31.15.ae, 61.72.S–, 62.20.–x **DOI:** 10.1088/1674-1056/27/3/037105

1. Introduction

Nickel aluminum (NiAl) intermetallics has a lot of attractive properties, such as high melting temperature, low density, good thermal conductivity, excellent corrosion, and oxidation resistance, so it is a good candidate for aerospace industry applications.[1–3] Its practical use, however, is limited by its poor ductility at low temperatures.[3] NiAl exists as polycrystals,[3] so the defects of grain boundaries (GBs) are inevitable in NiAl. The GBs in metals and alloys offers favorable sites for the segregation of impurities.[4]

Impurity such as P is one of the uncontrollable ingredients that can have strong effects on the mechanical properties of alloy.[5–10] However, there are few reports about the effects of P in NiAl intermetallics, especially for NiAl GB. For such a long period, P was considered as a deleterious element in superalloys and steels.[11,12] Nevertheless, more and more advantageous effects of P on superalloys and steels have been observed.[13] In order to improve the understanding of these effects, we considered the effect of P on the mechanical properties of NiAl and analyzed its micro mechanism.

In our previous study,[14] we demonstrated that impurity P prefers to segregate in NiAl GB rather than in NiAl bulk. In most part of the range of the permissible chemical potential, P atom tends to occupy interstitial site that is in the Ni-rich environment in NiAl GB; in the extremely Ni-rich environment in NiAl GB, P atom prefers to substitute Al atom that is the first nearest to GBs. Besides, there are interactions between P and Ni atoms, forming P–Ni bonds. The P–Ni covalent bonds might embrittle NiAl GB and be harmful to the plasticity of the NiAl intermetalllics. But the studies about the effect of P impurity on mechanical properties of NiAl GB are quite limited.

In this article we employ first-principle calculations to study the effect of P on mechanical properties of NiAl GB from the perspectives of "stress" and "energy". In the "stress" aspect, we use first-principle computational tensile test (FPCTT) in order to determine the ideal strength of NiAl GB. In the "energy" aspect, the cleavage energy and embrittlement potential are explored in this paper.

2. Computational methods

All calculations were based on the density functional theory (DFT) and ultra-soft pseudopotential as implemented in the Vienna ab initio simulation package (VASP).[15,16] We employed the generalized gradient approximation (GGA) according to the Perdew and Wang (PW91).[17] The 400 eV was used as a cutoff energy for the plane wave basis. The Brillouin zones were sampled with $2\times4\times8$ k points by Monkhorst–Pack scheme.[18] When a convergence criterion of the force on each atom was less than 10^{-3} eV/Å, all atomic positions were fully relaxed.

The selected NiAl Σ5 (310)/[001] tilt grain boundary is considered to be a typical coincidence boundary in NiAl, which is formed by rotating a grain 36.9° along the [001] axis

*Project supported by the National Natural Science Foundation of China (Grant Nos. 11404396 and 51201181) and the Subject Construction Fund of Civil Aviation University of China (Grant No. 000032041102).

†Corresponding author. E-mail: huxlemma@163.com

© 2018 Chinese Physical Society and IOP Publishing Ltd

and taking (310) as its boundary plane. The supercell of NiAl Σ5 GB we constructed is shown in Fig. 1, whose three dimensions are 19.38×9.10×5.65 Å^3. This supercell is set to contain four (001) atomic layers, including two Ni layers and two Al layers with 40 Ni atoms and 40 Al atoms respectively. To meet the periodic boundary condition, the supercell has two symmetric boundaries in the direction of [310]. For the direction of [001], the length of supercell is chosen to be twice the crystal super lattice (CSL) to keep the symmetry of the configuration.

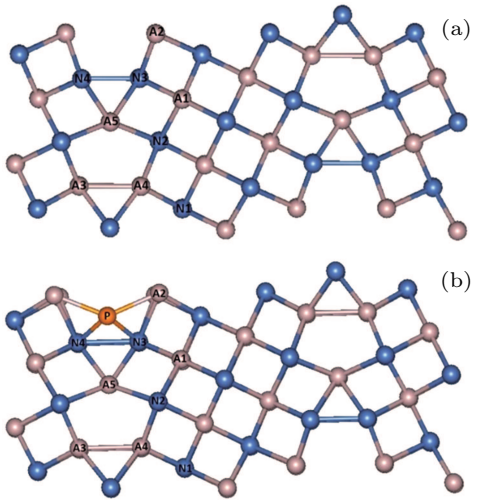


Fig. 1. (color online) Planforms of supercell of NiAlΣ5 (310)/[001] GB for (a) pure NiAl GB and (b) NiAl GB with P impurity.

For convenience, we numbere some atoms. A (A1, A2, A3, A4, and A5) represents Al atom, N (N1, N2, N3, and N4) represents Ni atom, P represents P atom. P atom is put at the most stable site in NiAl Σ5 GB.

To make sure that the supercell we constructed is large enough for P atom to be inserted into NiAl Σ5 GB, we calculate the solution energy of P in the interstitial site of NiAl GB by

$$E^{\mathrm{f}}_{\mathrm{nP}} = E^{\mathrm{T}}_{\mathrm{NiAl-nP}} - E^{\mathrm{T}}_{\mathrm{NiAl}} - nE_{\mathrm{P}}, \tag{1}$$

where $E^{\mathrm{T}}_{\mathrm{NiAl-nP}}$ and $E^{\mathrm{T}}_{\mathrm{NiAl}}$ represent the total energies of NiAl GB supercell with and without P, respectively; E_{P} refers to the energy of a single P atom and its value is equal to −0.17 eV. If we place one P atom into NiAl GB, the solution energy equals −5.70 eV. With one P placed in a GB and another placed in the other GB, the solution energy equals −11.43 eV, thus each P atom has an average of −5.71 eV. It means that there is no interaction between these two P atoms, and so, the supercell we constructed is large enough for P atom to be inserted into NiAl Σ5 GB.

3. Results and discussion

3.1. Cleavage energy

Fracture is the state that the deformation of the solid material is beyond the plastic limit under the action of the force, and the fracture of the material means the complete failure of the material. The crack propagation can be characterized by the cleavage energy of the crack plane.

We have constructed a model of brittle fracture at grain boundaries. In order to eliminate the interaction between these two fractured surfaces, we set a vacuum layer with a thickness of 9.69 Å between the fractured surfaces as shown in Fig. 2. The atoms that are the first nearest to the vacuum layer are fixed to prevent their movement.

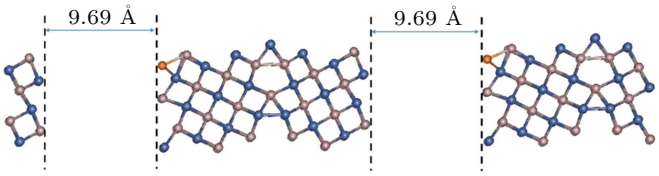


Fig. 2. (color online) Fracture surface with a vacuum of 9.69 Å in P–NiAl GB.

Cleavage energy γ_{C} is defined as the energy required to split the solid into two free surfaces. The value of cleavage energy γ_{C} is twice as great as surface energy γ_{S}. The calculation formula of cleavage energy γ_{C} is as follows:

$$\begin{aligned} \gamma_{\mathrm{C}} &= 2\gamma_{\mathrm{S}}, \\ \gamma_{\mathrm{S}} &= \frac{E_{\mathrm{S}} - E_0}{2\Delta s}, \end{aligned} \tag{2}$$

where E_{S} is the system energy with fractured surfaces, while E_0 is the system energy without fractured surfaces, and ΔS is the area of the fractured surface. According to the previous study, the values of E_0 are −413.13 eV for pure NiAl GB and −419.00 eV for P–NiAl GB, respectively. Through the first principle calculation, the cleavage energy values are 0.84 J/m^2 for pure NiAl GB and 0.79 J/m^2 for P–NiAl GB, respectively. That is to say, the cleavage energy of P–NiAl GB is less than that of pure NiAl GB, indicating that NiAl GB is easier to fracture with P segregating. Hence, we can deduce that P embrittles NiAl GB.

3.2. Embrittlement potential

The conception of embrittlement potential is proposed by Rice and Wang.[19] Embrittlement potential characterizes the mechanism of the metalloid-induced intergranular embrittlement through the competition between brittle boundary separation and plastic crack blunting. According to the model of Rice and Wang, the ability to segregate atom to reduce the brittle boundary fracture is linearly dependent on the difference in solution energy between the cases where the impurity is at the GB and at the free surface. In other words, if the solution energy of impurity at the free surface is larger than that at the GB, the impurity prefers to stay in GB and enhance the cohesion of GB. Oppositely, if solution energy of impurity at the

free surface is less than that at the GB, the impurity prefers to stay in free surface and GB is embrittled by impurity.

We remove the atoms from one side of GB, and constructe vacuum layer in the surface of (310) for NiAl and P–NiAl, separately (Fig. 3). The length of vacuum layer is 5 Å. The atoms which are the first nearest to the vacuum layer are fixed to prevent their movement.

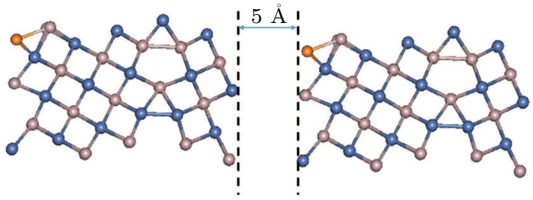


Fig. 3. (color online) Free surface with a vacuum 5 Å in P–NiAl GB.

The solution energy $E_{\mathrm{FS}}^{\mathrm{sol}}$ of P on the free surface is expressed as

$$E_{\mathrm{FS}}^{\mathrm{sol}} = E_{\mathrm{FS,P}}^{\mathrm{T}} - E_{\mathrm{FS}}^{\mathrm{T}} - E_{\mathrm{P}}, \tag{3}$$

where $E_{\mathrm{FS,P}}^{\mathrm{T}}$ and $E_{\mathrm{FS}}^{\mathrm{T}}$ are the total energies of NiAl(310) free surface supercell with and without P, respectively, E_{P} represents the energy of a single P atom and its value equals -0.17 eV. After calculation, the solution energy of NiAl Σ5 (310) free surface is -6.35 eV.

Based on Rice and Wang model, the sign of ΔE could determine the strengthening and embrittling effect of P impurity in NiAl Σ5 GB. Negative value of ΔE indicates embrittling, while positive one indicates strengthening. ΔE is expressed as

$$\Delta E = E_{\mathrm{FS}}^{\mathrm{S}} - E_{\mathrm{GB}}^{\mathrm{S}}. \tag{4}$$

According to the previous study, the solution energy $E_{\mathrm{GB}}^{\mathrm{S}}$ of P in NiAl GB at the most stable site is -5.70 eV.[14] Hence, ΔE is calculated to be -0.65 eV, which indicates that P prefers to stay in NiAl Σ5 (310) free surface rather than in NiAl GB. That is, P impurity embrittles the NiAl Σ5 GB.

3.3. Theoretical tensile strength

Theoretical toughness, Griffith fracture energy, and theoretical tensile strength can describe the mechanical properties of material. Through the first-principle computational tensile test of NiAl GB, theoretical toughness, Griffith fracture energy and theoretical tensile strength can be analyzed. Theoretical toughness and Griffith fracture energy are closely related to the total energy of the system.

The first-principle computational tensile test is conducted along the X axis (perpendicular to the direction of GB interface) in steps of 2% strain. The GB model for each tensile step is the optimized GB model of the last tensile step, which can ensure the continuity of the tensile process. In the GB tension model, we consider the Poisson effect, that is, the size of the YZ surface (GB interface) changes with the increase of strain.

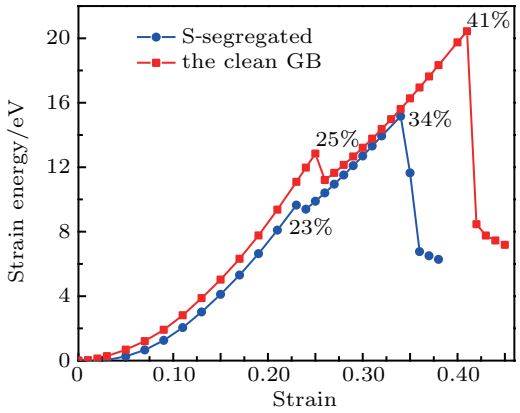


Fig. 4. (color online) Plots of system strain energy versus strain for NiAl and P–NiAl GB, obtained by FPCTT. The zero of strain energy is set to be the minimum energy of the system.

Figure 4 shows the plots of system strain energy versus strain for NiAl and P–NiAl GB. From Fig. 4 it follows that for pure NiAl Σ5 GB, the strain energy increases with the increase of tensile strain. When the strain reaches 25%, the strain energy reaches a maximum value of 12.84 eV first. After the strain of 25%, strain energy begins to decrease, reaching a minimum value of 11.2 eV at a strain of 26%. Then, the strain energy continues to increase gradually and reaches a second maximum of 20.4 eV at a strain of 41%. After the strain of 41%, the strain energy reduces sharply.

Like the scenario in the pure NiAl GB, the strain energy augments as the strain increases in P–NiAl GB, reaching its first maximum value of 9.6 eV at a strain of 23%.When the strain reaches 24%, the strain energy reduces to 9.4 eV. Then, the strain energy continues to increase gradually and reaches a second maximum of 15.2 eV at a strain of 34%. After the strain of 34%, the strain energy reduces sharply. Compared with the strain for pure NiAl GB, the strains for P–NiAl GB at the first and second maximum value of the strain energy are both less than those of the pure NiAl GB.

First-principle computational tensile test is based on first principle method. According to Nielsen-Martin's stress calculation theory,[20,21] the average system stress under different strains could be calculated by

$$\sigma_{\alpha\beta} = \frac{1}{\Omega}\frac{\partial E_{\mathrm{total}}}{\varepsilon_{\alpha\beta}}. \tag{5}$$

The formula can be defined as the partial differential of total energy E_{total} with respect to strain tensor $\varepsilon_{\alpha\beta}$, and then divided by the volume of cell Ω. As a consequence, the stress–strain curve can be obtained through the first-principle computational tensile test, and then the theoretical tensile strength of the material can be determined.

Figure 5 shows the plots of stress versus strain for NiAl and P–NiAl GB obtained by the first principle tensile test in the direction of (310). The red curve is for pure NiAl GB while the blue one represents P–NiAl GB. From Fig. 4, for pure NiAl

Σ5 GB, the stress augments with the increase of tensile strain. When the strain reaches 24%, the stress reaches a maximum value of 164.7 GPa first. At a strain of 25%, stress suddenly decreases to 83.6 GPa, which is corresponding to the decrease of strain energy. Then, as strain energy increases it increases gradually and reaches a second maximum of 133.7 GPa at a strain of 38%. At a strain of 41%, the stressdecreases sharply to −68.6 GPa, which corresponds to the decrease of strain energy.

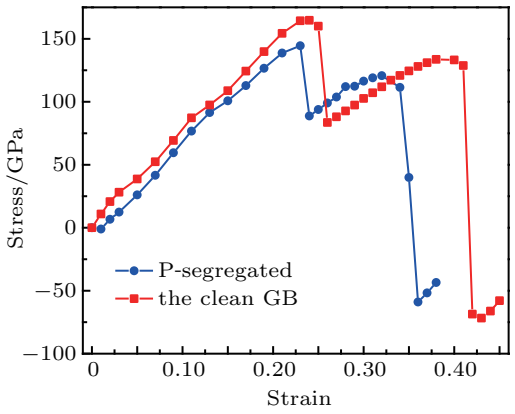


Fig. 5. (color online) Plots of stress versus strain for NiAl and P–NiAl GB, obtained by FPCTT.

Like the stress of the pure NiAl GB, the stress augments as the strain increases in P–NiAl GB, reaching its first maximum value of 144.5 GPa at a strain of 23%. When the strain reaches 24%, the strain energy decreases to 88.7 GPa, which is corresponding to the decrease of strain energy. Then, as strain energy continues to increase gradually and reaches a second maximum of 120.7 GPa at a strain of 32%. After a strain of 34%, the strain energy reduces sharply to 39.9 GPa, which corresponds to the decrease of strain energy. Compared with the strains for pure NiAl GB, the strains for P–NiAl GB at the first and second maximum value of the stress are both less than those of the pure NiAl GB. The first and second maximum value of stress in the pure NiAl GB are at the strains of 25% and 41%, while for P–NiAl GB, these two maximum values are at the strains of 23% and 34%, respectively. It is indicated that the extreme point is advanced with the addition of P atoms. That is, P atom embrittles NiAl GB. Moreover, the extreme value of P–NiAl is less than that of pure NiAl, demonstrating that the segregation of P atom reduces the theoretical tensile strength of NiAl GB.

3.4. Atomic bond length

In order to further analyze the causes of the extreme points of the strain energy–strain curves and stress–strain curve and to understand the fracture tensile process from the perspective of atoms, we analyze the changes of atom bond length near the boundaries.

Figures 6(a) and 6(b) show the bond length–strain curves of NiAl GB. According to Fig. 6(a), with the augment of strain, the bond lengths of N3N5, N3A1, and N3A2 are almost unchanged, while the bond length of N3N4 increases almost linearly. At the strain of 25%, the length of N3N4 increases sharply, reaching 3.89 Å (2.42 Å at a strain of 0), which shows the cleavage of N3N4 bond. In Fig. 6(b), there is little change of A5N3 bond length as strain increases, while the bond lengths of A3A4 and A5N2 increase almost linearly. When the strain reaches 25%, the bond length of A5N2 increases significantly from 2.62 Å at a strain of 0 to 4.79 Å at a strain of 25%, which means the cleavage of A5N2 bond. Hence, the first maximum value of stress is caused by the fracture of Ni–Ni bond (N3N4) and Al–Ni bond (A5N2). After the strain of 25%, the bond lengths of N3N4 and A5N2 continue to increase linearly, while other atomic bonds do not change much. Hence, the second maximum value of stress is also caused by the fractures of Ni–Ni bond (N3N4) and Al–Ni bond (A5N2).

Figures 6(c) and 6(d) show the the bond length–strain curves of P–NiAl GB. From Fig. 6(c) it follows that with the augment of strain, the bond lengths of N3N5, N3A1, and N3P are almost unchanged, while the bond length of N3N4 increases almost linearly. At strains of 23% and 34%, the length of N3N4 decreases significantly. We deduce that the decrease of N3N4 bond length is caused by the change of GB structure, which makes the N3N4 bond stronger. Compared with the scenario in Fig. 6(a), the segregation of P in NiAl GB strengthens the interaction between Ni–Ni bonds.

From Fig. 6(d) it can be seen that A5N2 and A5N3 bond length have little changes as the strain increases, while the bond length of A3A4 increases almost linearly. When the strain reaches 23%, the bond length of A3A4 increases significantly from 2.63 Å at the strain of 0 to 4.85 Å at the strain of 23%, which means the cleavage of A3A4 bond. After the strain of 23%, the bond length of A3A4 continues to increase linearly. Therefore, the first and second maximum values of stress are both caused by the fracture of Al–Al bond (A3A4).

Figure 7 shows the variations of bond length between P and its first closest atoms with strain in P–NiAl GB. As shown in Fig. 7, with the increase of strain, there is little change of PN4 bond length, and the bond length of PA5 decreases slightly. However, PA5 bond length increases significantly at a strain of 35%, reaching 4.41 Å (2.91 Å at the strain of 0). In addition, the bond length of PA2 increases linearly with the augment of stain. At the stain of 35%, bond length of PA2 reaches 7.58 Å (2.40 Å at the strain of 0), which means the cleavage of PA2 bond. Therefore, the second maximum of stress of P–NiAl GB is caused by the cleavage of P–Al bond (PA2).

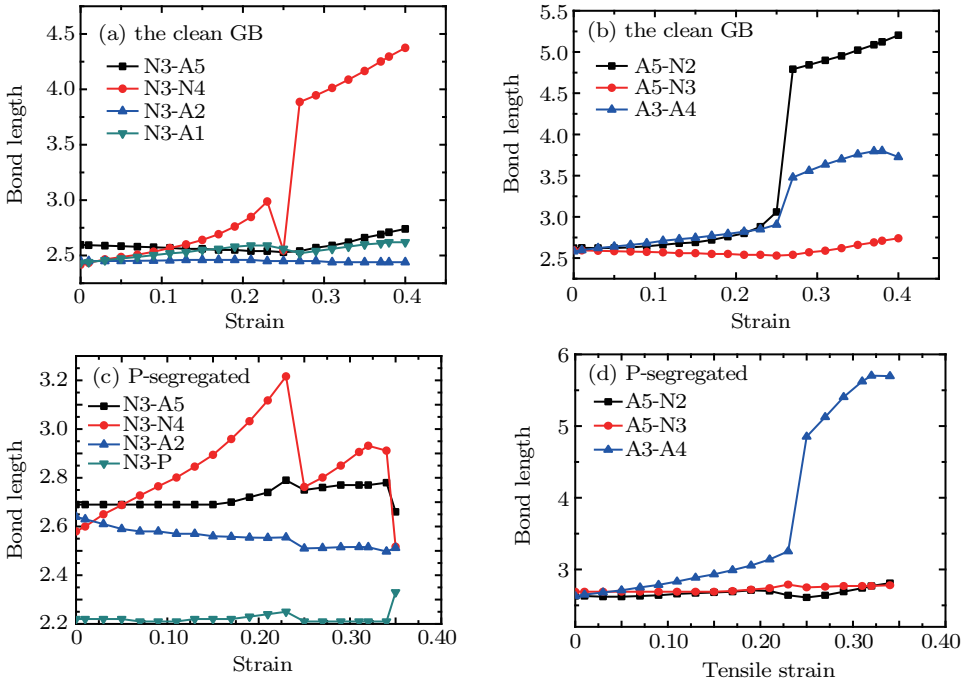


Fig. 6. (color online) Plots of atomic bond length versus tensile strain of NiAl and P–NiAl GB.

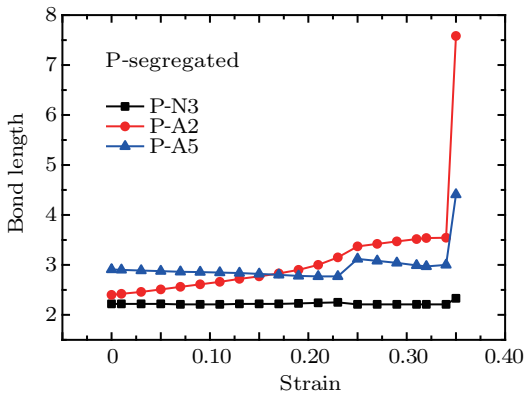


Fig. 7. (color online) Plots of atomic bond (P and its first closest atoms) length versus tensile strain for P-N3, P-A2, and P-A5.

Above all, the fracture of pure NiAl GB is caused by the cleavages of Ni–Al and Ni–Ni bond, while the cleavages of Al–Al bond and P–Al bond cause the P–NiAl GB to fracture. Thus, we can deduce that the segregation of P in NiAl GB can weaken the interaction between Al–Al bonds and P–Al bonds.

3.5. Charge density

The deformation charge density is used to investigate the bonding between atoms, which shows the distribution of charge density and the movement of the electrons around the atoms. The weakening and strengthening of chemical bonds are characterized by charge depletion and accumulation, respectively. In order to more in depth understand the interactions between P–Ni atoms and between P–Al atoms, we study the deformation charge density. The charge density difference $\Delta\rho$ is calculated from

$$\Delta\rho = \rho_{\mathrm{NiAl-P}} + \rho_{\mathrm{NiAl,without.Ni}} - \rho_{\mathrm{NiAl}} - \rho_{\mathrm{NiAl-P,without.Ni}}, \quad (6)$$

where $\rho_{\mathrm{NiAl-P}}$ represents the charge density of NiAl GB with P segregated in the GB, $\rho_{\mathrm{NiAl,without.Ni}}$ is the charge density of NiAl GB without Ni atom, ρ_{NiAl} is the charge density of pure NiAl GB, and $\rho_{\mathrm{NiAl-P,without.Ni}}$ is the charge density of NiAl GB with P segregated in the GB and without Ni atom.

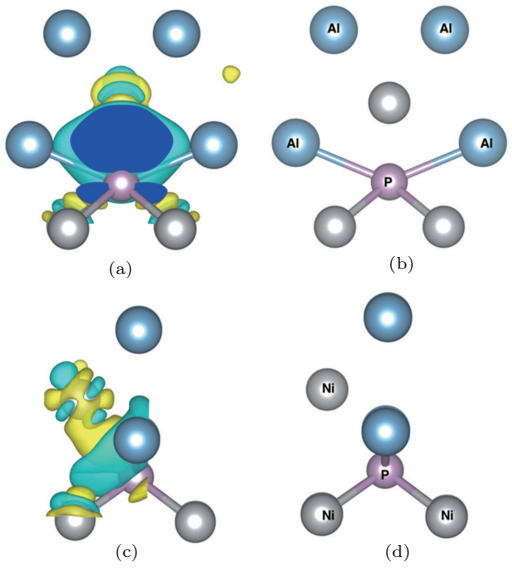


Fig. 8. (color online) (a) Deformation charge density between P and Al, (b) atomic structure corresponding to (a), (c) deformation charge density between P and Ni, and (d) atomic structure corresponding to (c). Yellow area represents the charge accumulation and the green part indicates the charge depletion.

From Fig. 8, we can see that there is an obvious charge accumulation between P atom and Ni atoms, indicating that the interaction between P atom and Ni atom is stronger. We can also see the charge depletion between P atom and Al atoms,

indicating the weakness of P–Al interaction. Also the interaction between Al–Al bonds is weakened. From this analysis we can explain why the fracture of P–NiAl GB is caused by the cleavages of Al–Al and P–Al bond.

4. Conclusions

The cleavage energy for pure NiAl GB goes to 0.84 J/m^2 while 0.79 J/m^2 for P–NiAl GB. In other words, the cleavage energy of P–NiAl GB is less than that of pure NiAl GB, indicating that the NiAl GB is easier to fracture with P segregating. So we can conclude that P embrittles the NiAl GB. According to Rice and Wang's model, the embrittlement potential is calculated to be -0.65 eV, which indicates that P prefers to stay in NiAlΣ5 (310) free surface rather than in NiAl GB. That is to say, P impurity embrittles the NiAlΣ5 GB.

According to the first-principle computational tensile test, P–NiAl GB fractures at a strain of 34%. The fractured strain of P–NiAl GB is less than the one of pure NiAl GB (41%), which means that the segregation of P in NiAl GB makes the GB easier to fracture than in pure GB. Besides, the maximum stress of P–NiAl GB (144.5 GPa) is less than that of pure NiAl GB (164.7 GPa). In other words, P reduces the theoretical tensile strength of NiAl GB. The fracture of pure NiAl GB is caused by the cleavages of Ni–Al and Ni–Ni bond, while the cleavage of Al–Al bond causes the P–NiAl GB to fracture. Thus, we can deduce that the segregation of P in NiAl GB weakens the interaction between Al–Al bonds and strengthens the interactions between Ni–Al bonds and between Ni–Ni bonds. Our calculations clarify the effects of P on the mechanical properties of the NiAl GB, and these results will provide a good reference for selection, preparation and application of the NiAl intermetallics.

The study of microscopic structure through first-principle calculations is of great significance for understanding the macroscopic mechanical properties. Our methods using both "stress" and "energy" for NiAl can also be reasonably generalized to other structural materials such as intermetallics as well as metals and alloys.

References

[1] Stoloff N S 2009 *Microstructure and Properties of Materials,* Vol. 1 (Singapore: World Scientific) pp. 51–106
[2] Miracle D B 1993 *Acta Metall. Mater.* **41** 649
[3] Miracle D B and Darolia R 1995 *Intermetallic Compounds: Principles and Practice*, Vol. 2 (Chichester: Wiley) pp. 53–72
[4] Zhou H B, Jin S, Zhang Y and Lu G H 2011 *Sci. China Phys. Mech. Astron.* **54** 2164
[5] Liu L H, Zhang Y, Hu X L and Lv G H 2009 *J. Phys. Condens. Matter* **21** 015002
[6] Liu C T, White C L and Horton J A 1985 *Acta Metall.* **33** 213
[7] Jayaram R and Miller M K 1993 *Appl. Surf. Sci.* **67** 311
[8] Miller M K, Anderson I M and Russell K F 1996 *Appl. Surf. Sci.* **94** 288
[9] Jayaram R and Miller M K 1995 *Scripta Metallurgicaet Materialia* **33** 119
[10] Zhang G Y, Guo J T and Zhang H 2007 *Meter. Eng.* **4** 43
[11] Sun W R, Guo S R and Lu D Z 1997 *Metal. Mater. Trans.* **28A** 649
[12] Zhou J and Guo J T 2004 *Acta Metall. Sin.* **40** 67 (in Chinese)
[13] Zhang G Y, Guo J T and Zhang H 2007 *Meter. Eng.* **4** 43 (in Chinese)
[14] Hu X L, Zhao R X, Luo Y and Song Q G 2017 *Chin. Phys. B* **26** 023101
[15] Kresse G and Hafner J 1993 *Phy. Rev. B* **47** 558
[16] Kresse G and Furthmuller J 1996 *Phy. Rev. B* **54** 11169
[17] Perdew J P and Wang Y 1992 *Phys. Rev. B* **46** 12947
[18] Monkhorst H J and Pack J D 1976 *Phys. Rev. B* **13** 5188
[19] Rice J R and Wang J S 1989 *Mater. Sci. Engi. A* **107** 23
[20] Roundy D and Cohen M L 2001 *Phys. Rev. B* **64** 212103
[21] Ogata S, Li J and Yip S 2002 *Science* **298** 807